Chapter 6
Bremsstrahlung of Fast Charged Particles with an Electron Core in a Medium

6.1 Polarization Bremsstrahlung of a Hydrogen-Like Ion in a Crystal

6.1.1 Introductory Remarks

In scattering of a fast ion in a medium, ordinary (static) bremsstrahlung caused by acceleration of an incident particle (IP) in the field of a target is suppressed because of the high mass of an ion. So the prevailing mechanisms of photon emission in this case are connected with excitation (real or virtual) of electronic degrees of freedom of colliding particles. In emission of high-energy photons with an energy of the order of the IP kinetic energy, when a momentum transferred in collision is great in comparison with the characteristic momenta of bound electrons, considered as main mechanisms of radiation, as a rule, are processes with changing state of an electron subsystem. Among these processes are radiation ionization, emission of secondary electrons, and radiation electron capture [1]. In the spectral region far from the kinematic limit, when the characteristic transferred momentum is not great, and the photon frequency is of the order of the frequencies of excitation of bound electrons of colliding particles, it is necessary to take into account radiation caused by virtual excitation of electronic degrees of freedom without change of an electronic state. This kind of radiation defined by the dynamic polarizability of a target and an IP was called polarization bremsstrahlung [2].

PBs is a fundamental radiative process representing the conversion of the electromagnetic eigenfield (a virtual photon) of one of colliding particles to a real photon on the electron shell of another particle. In the case that both particles have electronic degrees of freedom, radiation can proceed by two channels according to on whose bound electrons the conversion of a virtual photon occurs. Thus, generally speaking, "target" PBs caused by the polarizability of target atoms (channel 1) and PBs of an incident particle caused by virtual excitation of an IP electron (channel 2) take place. The schematic representation of two PBs channels is shown in Fig. 6.1. It should be noted that the first PBs channel was studied by different authors both for a

V. Astapenko, *Polarization Bremsstrahlung on Atoms, Plasmas, Nanostructures and Solids*, Springer Series on Atomic, Optical, and Plasma Physics 72,
DOI 10.1007/978-3-642-34082-6_6,

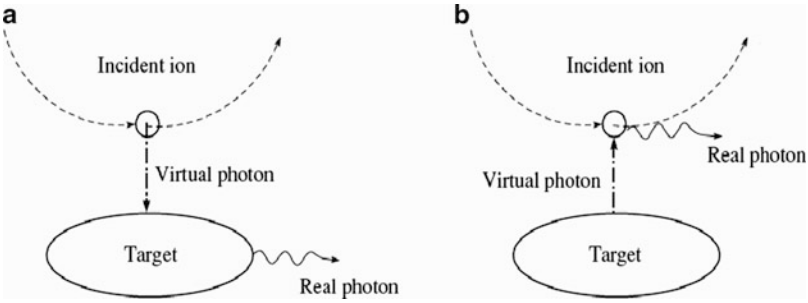

Fig. 6.1 (**a**) PBs by the first channel (target PBs), (**b**) PBs by the second channel (PBs from an IP)

case of collision of a pair of particles and in scattering in a medium [3–8]. The role of the second PBs channel is studied much less. Both PBs channels were first calculated in the works of M.Ya. Amus'ya with co-authors [2, Chap. 7].

In going to consideration of PBs of an ion with an electron core in a crystal, it is necessary to take into account collective effects caused by a possibility of coherent interaction of an IP with a target. This problem becomes especially urgent in connection with further improvement of methods of producing fast ion beams with specified characteristics including beams of multiply charged hydrogen-like ions [1]. Various aspects of interaction of such ions with a substance have been intensively studied in recent years [9, 10]. In particular, coherent excitation of a hydrogen-like argon ion in a single crystal was investigated experimentally [11], in which a momentum multiple of the momentum of a reciprocal lattice is transferred to a target (the Okorokov effect). Since PBs can be considered as a process of virtual excitation of a subsystem of bound electrons with their following radiation deexcitation, it is natural to expect that coherent effects such as the Okorokov effect are to show themselves in polarization bremsstrahlung as well.

6.1.2 Bremsstrahlung in a Polycrystal

The expression for PBs on a target due to virtual excitation of a medium electron in a polycrystal was derived in [5]. In this case the frequency-angular distribution of photon yield per unit length is given by the sum of the incoherent and coherent contributions:

$$\frac{dN_t}{dl\, d\omega\, d\Omega_{\mathbf{k}}} = \frac{dN_t^{(incoh)}}{dl\, d\omega\, d\Omega_{\mathbf{k}}} + \frac{dN_t^{(coh)}}{dl\, d\omega\, d\Omega_{\mathbf{k}}}. \tag{6.1}$$

Incoherent PBs on a target is described by the formula:

$$\frac{dN_t^{(incoh)}}{dl\, d\omega\, d\Omega_{\mathbf{k}}} = 2\, n_t\, \frac{e^2}{\hbar\,\omega}\, \frac{\left|\omega^2 \alpha_t(\omega)\right|^2}{\pi\, \mathrm{v}^2\, c^3} \times$$
$$\times \int\limits_{q_{\min}}^{q_{\max}} \left(1 - \exp\left(-u^2\, q^2\right)\right) \left[Z_{proj} - F_{proj}(q_{1c})\right]^2 F_t^2(q)\, I\varphi(q, \mathrm{v}, \omega, \theta)\, \frac{dq}{q}, \qquad (6.2)$$

where $n_t, \alpha_t(\omega), F_t(q)$ are the concentration, the dynamic polarizability, and the form factor of target atoms; $\mathbf{v}, Z_{proj}, F_{proj}$ are the velocity, the nuclear charge number, and the form factor of an incident ion (IP); $\omega, \mathbf{k}$ are the frequency and the wave vector of radiation in the target rest frame, θ is the angle between $\mathbf{v}$ and $\mathbf{k}$ in the same rest frame; $\hbar\mathbf{q}$ is the momentum transferred from an IP to the target, $\hbar\mathbf{q}_1$ is the change of the IP momentum, $\hbar\mathbf{q}_{1c}$ is the same value in the IP rest frame; u is the root-mean-square deviation of target atoms from the equilibrium position; c is the velocity of light; $q_{\min} = (1 - (\mathrm{v}/\mathrm{c})\, \cos\theta)\, (\omega/\mathrm{v}), q_{\max} = 2\,\mu\,\mathrm{v}$, μ is the target IP reduced mass;

$$I\varphi(q, \mathrm{v}, \omega, \theta) = \frac{q^3\, \mathrm{v}}{2\,\pi} \int d\Omega_{\mathbf{q}}\, \delta(\omega - \mathbf{k}\mathbf{v} + \mathbf{q}\mathbf{v})\, \frac{\left[\mathbf{s}, \omega\, \mathbf{v}/c^2 - \mathbf{q}\right]^2}{\left(\mathbf{q}^2 - 2\, \mathbf{k}\, \mathbf{q}\right)^2},\ \mathbf{s} = c\, \mathbf{k}/\omega, \quad (6.3)$$

is the integral with respect to the solid angle connected with the momentum transfer vector. This integral in the nonrelativistic limit takes the form

$$I\varphi(q, \mathrm{v}{<<}c, \omega, \theta) \cong \frac{1 + \cos^2\theta}{2} + \left(\frac{\omega}{q\,\mathrm{v}}\right)^2 \frac{1 - 3\cos^2\theta}{2}. \qquad (6.3a)$$

The formula (6.2) describes PBs on a target without excitation of bound electrons of the target and an IP – so-called "elastic" PBs.

The coherent part of PBs on a target is given by the following expression [5]:

$$\frac{dN_t^{(coh)}}{dl\, d\omega\, d\Omega_{\mathbf{k}}} = 2\, n_t^2\, \frac{e^2}{\hbar\,\omega}\, \frac{\left|\omega^2\ \alpha_t(\omega)\right|^2}{\pi\, \mathrm{v}^2\, c^3} \sum_g N(g)\ \Theta\left(g\mathrm{v} - \omega\left(1 - \frac{\mathrm{v}}{\mathrm{c}}\cos\theta\right)\right) \times$$
$$\times \frac{\exp(-u^2\, g^2)}{g^3}\, F_t^2(g)\, I\varphi(g, \mathrm{v}, \omega, \theta) \int\limits_0^{2\pi} \left[Z_{proj} - F_{proj}(g_{1c}(\phi))\right]^2 d\phi\ . \quad (6.4)$$

There is the sum over the magnitudes of the reciprocal lattice vectors $\mathbf{g}$, $N(g)$ is the number of these vectors with a specified magnitude g; φ is the azimuth angle of $\mathbf{g}$. In Eq. 6.4 averaging over the $\mathbf{g}$ direction is made to describe the contribution of all polycrystalline cells to the process. The theta function $\Theta(x)$ expresses the law of conservation of energy-momentum in radiation.

The expression for PBs of an IP (projectile) in a polycrystal can be derived with the use of the approach proposed in [2, Chap. 7] for description of PBs in atom-atom

collisions in the relativistic case. Generalization of this approach to scattering in a polycrystalline medium gives the following expression for the incoherent channel:

$$\frac{dN_{proj}^{(incoh)}}{dl\, d\omega\, d\Omega_{\mathbf{k}}} = n_t \frac{e^2}{\hbar\,\omega} \frac{\left|\omega\,\omega_c\,\alpha_{proj}(\omega_c)\right|^2}{\pi\,\mathrm{v}^2\,c^3}\left(1+\cos^2\theta_c\right)\times$$
$$\times \int\limits_{q_{\min}}^{q_{\max}} F_{proj}^2(q_{1c})[Z_t - F_t(q)]^2\left(1-\exp\left(-u^2\,q^2\right)\right)\frac{dq}{q}, \tag{6.5}$$

where $\alpha_{proj}(\omega_c)$ is the dynamic polarizability of an IP at the frequency in the IP rest frame and θ_c as a radiation angle in the IP rest frame. These values are connected with their analogs in the target rest frame according to the relations:

$$\omega_c = \gamma\,\omega\,(1-(\mathrm{v}/c)\,\cos\theta),\ \cos\theta_c = \frac{\cos\theta - \mathrm{v}/c}{1-(\mathrm{v}/c)\,\cos\theta}, \tag{6.6}$$

where $\gamma = 1/\sqrt{1-(\mathrm{v}/c)^2}$..

The coherent channel of PBs of an IP is described by the formula:

$$\frac{dN_{proj}^{(coh)}}{dl\, d\omega\, d\Omega_{\mathbf{k}}} = n_t^2 \frac{e^2}{\hbar\,\omega} \frac{\left|\omega\,\omega_c\,\alpha_{proj}(\omega_c)\right|^2}{\pi\,\mathrm{v}^2\,c^3}\left(1+\cos^2\theta_c\right)\times$$
$$\times \sum_g N(g)\ \Theta\left(g\mathrm{v} - \omega\left(1-\frac{\mathrm{v}}{\mathrm{c}}\cos\theta\right)\right)\frac{\exp(-u^2\,g^2)}{g^3}$$
$$\times\ [Z_t - F_t(g)]^2 \int\limits_0^{2\pi} F_{proj}^2(g_{1c}(\phi))\,d\phi\,. \tag{6.7}$$

Total PBs on an IP is given by the sum of Eqs. 6.5 and 6.7 as in the case of PBs on a target Eq. 6.1.

Let us consider a hydrogen-like incident ion. The eigenfrequencies of its bound electrons are given by the Bohr formula (the initial state of an IP electron is supposed to be the ground state):

$$\omega_n = Z_{proj}^2\,Ry\left(1-n^{-2}\right), \tag{6.8}$$

where Ry =13.6 eV and n is the principal quantum number. The IP form factor is

$$F_{proj}(q_1) = \frac{1}{\left(1+\left(a_{proj}\,q_1/2\right)^2\right)^2}, \tag{6.9}$$

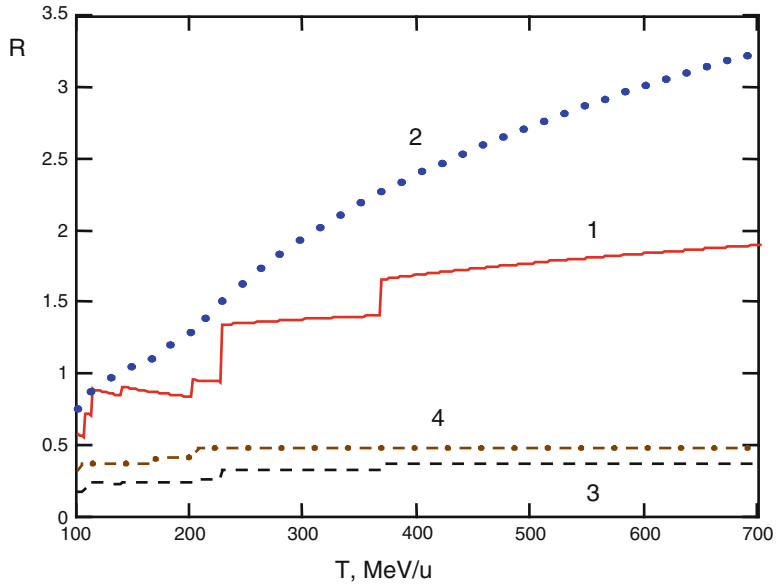

Fig. 6.2 The ratio between the coherent and incoherent contributions to PBs of an incident Ar^{17+} ion in aluminum: *1* – PBs on a target ($\theta = \pi/2$); *2* – PBs on a target ($\theta = \pi/6$); *3* – PBs on an IP ($\theta = \pi/2$); *4* – PBs on an IP ($\theta = \pi/6$)

where $a_{proj} = \hbar^2 / \left(Z_{proj}\, m\, e^2\right)$ is the Bohr radius. The general expression for the dynamic polarizability of an IP has the usual form:

$$\alpha_{proj}(\omega_c) = \frac{e^2}{m} \sum_n \frac{f_n}{\omega_n^2 - \omega_c^2}, \tag{6.10}$$

where f_n are the oscillator strengths that in case of a hydrogen-like ion have universal values independent of the charge number Z_{proj}. Small imaginary additives in the denominators on the right side of the Eq. 6.11 are omitted since further we do not consider the exact resonance when $\omega_c = \omega_n$.

At first, let us compare the contributions of the coherent and incoherent channels to PBs on a target and an IP. Figure 6.2 demonstrates this comparison for two values of radiation angles in case of scattering of a hydrogen-like argon ion in polycrystalline aluminum ($R = dN^{(coh)} / dN^{(incoh)}$).

The ratio R in Fig. 6.2 is shown as a function of the IP kinetic energy T for the specified photon energy $\hbar\omega = 6$ keV. The curves 1, 2 correspond to PBs on a target, the curves 3, 4 correspond to PBs on an IP. It can be seen from Fig. 6.2 that in case of PBs on a target the coherent channel prevails over the incoherent channel ($R > 1$), while for PBs on an IP there is an opposite situation ($R < 1$). The latter is due to the fact that in case of PBs on an IP an incident ion should approach the target nucleus to interact with it. But at such small distances the coherent interaction

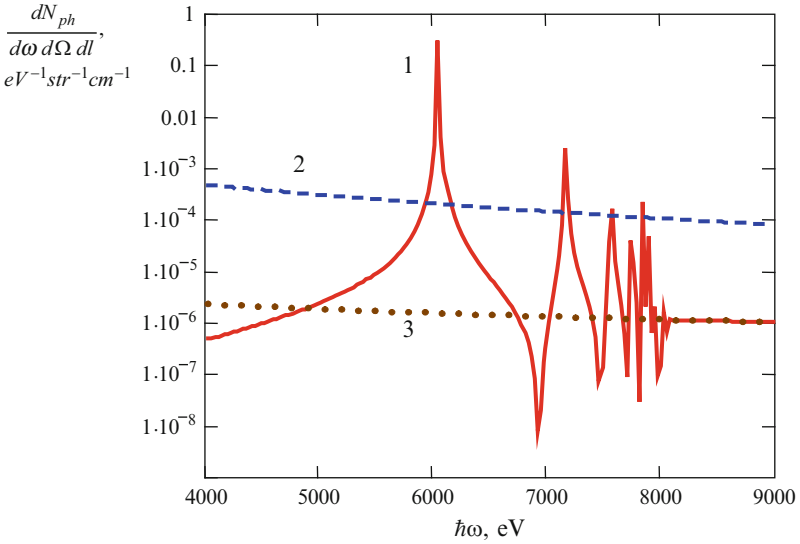

Fig. 6.3 The spectra of PBs of an Ar^{17+} ion in polycrystalline aluminum: *1* – PBs on an IP, *2* – PBs on a target, *3* – electron bremsstrahlung; T = 390 MeV/u ($\gamma = 1.42$), $\theta = \pi/6$

between an IP and the solid target is weak. During PBs on a target an incident ion interacts with target electrons. This interaction occurs at long distances (if the radiation frequency is not very high), so then coherent IP scattering by the target is strong enough. Coherent PBs leads to appearance of a distinct stepped structure on the curve 1. This structure is due to the presence of theta functions in the formulas (6.4), (6.7) that correspond to turning of the additional reciprocal lattice vector in the process with increasing IP kinetic energy.

Figure 6.3 demonstrates the spectra of PBs of an Ar^{17+} ion scattered in polycrystalline aluminum for the IP (curve 1) and target (curve 2) channels. There is also the spectrum of electron bremsstrahlung on the same target (curve 3).

In Fig. 6.3 the presence of sharp and relatively wide maxima in the spectrum of PBs on an IP can be seen (curve 1). These maxima correspond to fulfilment of the resonant conditions in the denominators of the expression for the dynamic polarizability of an IP (Eq. 6.10) in case of a hydrogen-like incident particle. Due to the Doppler effect (the first equation in Eq. 6.6), the resonance frequencies in the laboratory reference system depend on the IP energy and the radiation angle according to the formula

$$\omega_{\max}(n, \mathrm{v}, \theta) = \frac{\omega_n}{\gamma\,(1 - (\mathrm{v}/c)\,\cos\theta)}, \tag{6.11}$$

where ω_n is the eigenfrequency of a bound electron of an IP (Eq. 6.8), γ is the Lorentz factor. The first spectral maximum in Fig. 6.3 corresponds to virtual excitation of an IP electron to the excited state with $n = 2$. According to the formula (6.11), the resonant photon energy in this case (for specified values of T and θ) is

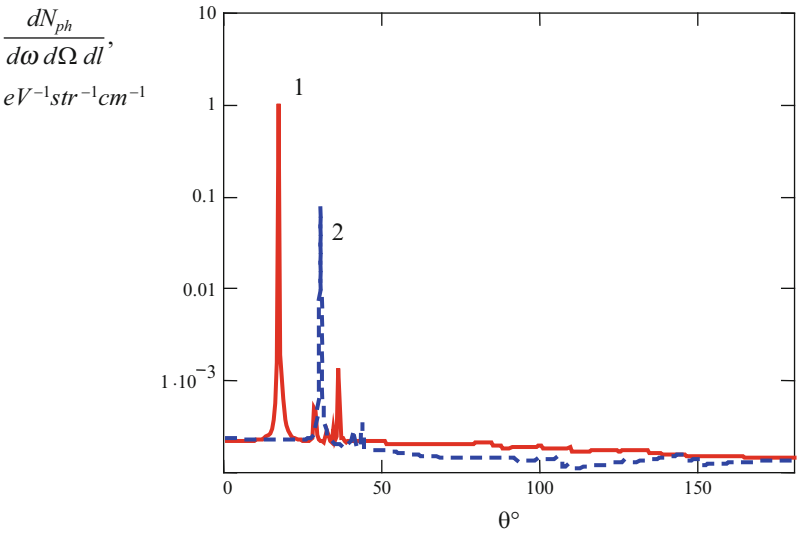

Fig. 6.4 The angular dependence of PBs on scattering of an Ar^{17+} ion in polycrystalline aluminum, $\hbar\omega = 6$ keV: *1* – T = 100 MeV/u, *2* – T = 390 MeV/u

6,041 eV, while in the IP rest frame it is equal to 3,305 eV. As can be seen from Fig. 6.3, in the vicinity of the maxima PBs on an IP strongly prevails over PBs on a target and electron bremsstrahlung. In the high-frequency limit the curves 1 and 3 coincide. This has a simple physical interpretation. A bound electron interacts with high-frequency radiation as a quasi-free electron. Therefore scattering of the IP eigenfield by an IP electron to a real high-energy photon occurs as by a free electron.

The angular dependence of PBs on scattering of an Ar^{17+} ion in polycrystalline aluminum ($\hbar\omega$ =6 keV) is shown in Fig. 6.4 for two values of IP kinetic energy.

There are also sharp maxima due to dependence of the resonance frequency in the target reference system on the radiation angle (Eq. 6.11). Radiation angles corresponding to the maxima in the angular PBs distribution are given by the formula:

$$\theta_{\max}(n,\omega,\mathrm{v}) = \arccos\left\{\frac{c}{\mathrm{v}}\left(1-\frac{\omega}{\gamma\,\omega_n}\right)\right\}, \tag{6.12}$$

where ω_n is the eigenfrequency of an IP electron (Eq. 6.8). It can be seen from Fig. 6.4 that the angles of the maxima increase with increasing IP kinetic energy.

Presented in Fig. 6.5 is PBs from hydrogen-like argon as a function of the IP kinetic energy for two values of the radiation angle. There are also sharp maxima in these dependences that have the same reason as in the case of the spectral-angular distribution of PBs. In this case, however, the first excitation frequency (Eq. 6.8) (n = 2) in the sum (Eq. 6.10) corresponds to the high-energy peaks on the curves 1, 2.

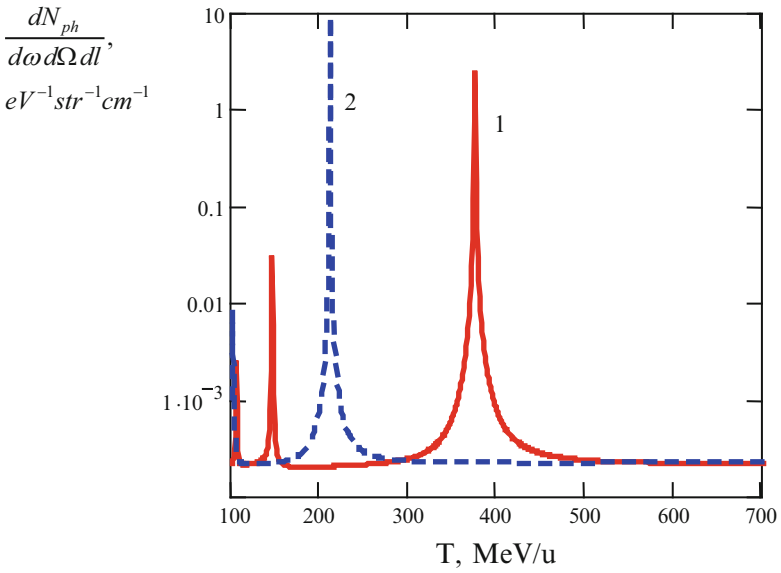

Fig. 6.5 PBs from an Ar^{17+} ion in polycrystalline aluminum as a function of the IP kinetic energy, $\hbar\omega = 6$ keV: *1* – $\theta = \pi/6$, *2* – $\theta = \pi/10$

This is due to the fact that the radiation frequency in the IP rest frame decreases with increasing IP kinetic energy according to the first formula (6.6).

It is shown that scattering of a fast multiply charged hydrogen-like ion in a polycrystalline target results in intense radiation that has a sharp frequency and angular dependence. This radiation arises due to scattering of the electromagnetic eigenfield of a target to a real photon by a bound electron of an IP (IP polarization bremsstrahlung). The PBs channel studied earlier due to scattering of the IP field to a real photon by target electrons may be called PBs on a target. In contrast to PBs on a target, the main contribution to PBs on an IP is made by the incoherent channel of the process. In this item it is demonstrated that the frequency-angular features of PBs on an IP strongly depend on the IP energy.

6.1.3 Bremsstrahlung in a Single Crystal

In this section we will consider a situation when a fast hydrogen-like ion with the velocity **v** is scattered in a single crystal and emits a PBs photon with the wave vector **k** in the geometry shown in Fig. 6.6.

The axes of the Cartesian coordinate system presented in this figure coincide with the crystallographic axes of the target. The ion velocity is supposed to be high enough, so that the first Born approximation for interaction of an IP with the target can be used. As was mentioned at the beginning of Chap. 6, in the case under consideration PBs proceeds by two channels: Eq. 6.13 due to virtual excitation of target electrons and Eq. 6.14 as a result of virtual excitation of the electron core of

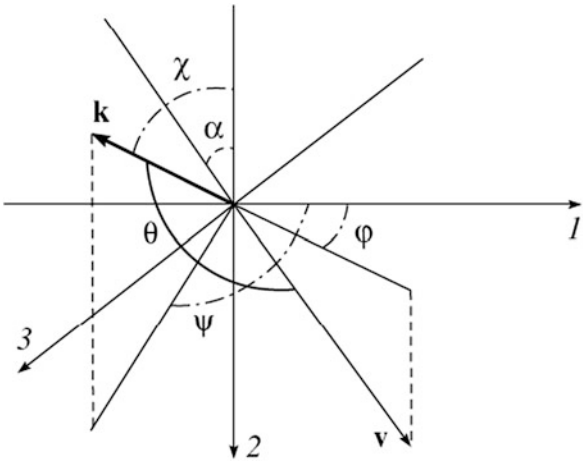

Fig. 6.6 The geometry of the process

an IP. In the first case scattering of the electromagnetic eigenfield of an incident ion to a real photon by target electrons occurs, and in the second case, on the contrary, there is scattering of the target eigenfield to a real photon by the electron core of an IP (Fig. 6.1). The expressions for the cross-sections of these channels can be obtained by summation of the contributions of PBs on different atoms (ions) of a substance. In the case under consideration with a crystalline target for each of the channels two types of the process are possible: the coherent process, when a momentum from an incident particle is transferred to the crystal lattice as a whole, and the incoherent process in case of pair interaction of an IP with atoms (ions) of a medium. Thus there are four kinds of PBs in consideration: coherent PBs on a target and an IP and incoherent PBs on a target and an IP.

To estimate the PBs value, it is convenient instead of the cross-section to use the number of photons emitted by an IP per unit length in the unit frequency range and to the unit solid angle. Then for coherent PBs by the first channel (Fig. 6.1a) the following expression can be obtained:

$$\frac{dN_t^{(coh)}}{dl\, d\omega\, d\Omega_{\mathbf{k}}} = \frac{n_t^2\, e^2}{\pi\, \hbar\, \mathrm{v}\, c^3} \sum_{\mathbf{g}} S^2(\mathbf{g})\ \delta(\omega + \mathbf{g}\mathbf{v} - \mathbf{k}\mathbf{v})\, \omega^3\, |\alpha_t(\omega)|^2 \times$$

$$\times \exp\left(-u^2\, g^2\right) \tilde{F}_t^2(g)\, \left[Z_{proj} - F_{proj}(g_{1c})\right]^2\, \frac{\left[\mathbf{s}, \omega\, \mathbf{v}/c^2 - \mathbf{g}\right]^2}{\left(\mathbf{g}^2 - 2\, \mathbf{k}\, \mathbf{g}\right)^2}. \quad (6.13)$$

Here the following designations are introduced: n_t is the concentration of target atoms, e is the elementary charge, c is the velocity of light, $S(\mathbf{g})$ is the geometrical structure factor of the crystal, $\mathbf{g}$ is the reciprocal lattice vector, ω is the frequency of a bremsstrahlung photon, $\alpha_t(\omega)$ is the dynamic polarizability of target atoms, u is the root-mean-square deviation of target atoms from the equilibrium position, $\tilde{F}_t(q)$ is the normalized form factor of medium atoms, Z_{proj} is the charge number of the IP nucleus, $F_{proj}(q)$ is the form factor of the IP electron core, $\mathbf{s} = c\,\mathbf{k}/\omega$ is the unit

vector in the direction of photon emission, $\mathbf{g}_1 = \mathbf{g} - \mathbf{k}$, $\mathbf{g}_{1c}$ is the reciprocal lattice vector in the reference system connected with an IP.

In derivation of the formula (6.13) integration with respect to the transferred wave vector $\mathbf{q}$ was performed in view of interaction of an IP with the target, which resulted in the equation $\mathbf{q} = \mathbf{g}$. The squared concentration of target atoms on the right side of the Eq. 6.13 is indicative of the coherent behavior of the process. The presence of the dynamic polarizability of target atoms in the formula (6.13) reflects the fact that photon emission results from induction of a variable dipole moment in target atoms during IP scattering. From the obtained expression it follows also that in the limit $u\,g > 1$ coherent PBs is low since then the coherence of IP interaction with a crystal lattice is violated.

The expression for incoherent PBs by the first channel looks like:

$$\frac{dN_t^{(incoh)}}{dl\,d\omega\,d\Omega_{\mathbf{k}}} = 2\,n_t\,\frac{e^2}{\hbar\,\omega}\,\frac{\left|\omega^2\alpha_t(\omega)\right|^2}{\pi\,\mathrm{v}^2\,c^3}\int\limits_{q_{\min}}^{q_{\max}}\left(1-\exp\left(-u^2\,q^2\right)\right)$$
$$\left[Z_{proj} - F_{proj}(q_{1c})\right]^2\,\tilde{F}_t^2(q)\,I\phi(q,\mathrm{v},\omega,\theta)\,\frac{dq}{q}, \tag{6.14}$$

where $q_{\min} = (1-(\mathrm{v}/\mathrm{c})\,\cos\theta)\,(\omega/\mathrm{v})$, $q_{\max} = 2\,\mu\,\mathrm{v}/\hbar$ are the minimum and maximum transferred vectors, μ is the reduced mass of an IP and an electron,

$$I\phi(q,\mathrm{v},\omega,\theta) = \frac{q^3\,\mathrm{v}}{2\,\pi}\int d\Omega_{\mathbf{q}}\,\delta(\omega - \mathbf{k}\mathbf{v} + \mathbf{q}\mathbf{v})\,\frac{\left[\mathbf{s},\,\omega\,\mathbf{v}/c^2 - \mathbf{q}\right]^2}{\left(\mathbf{q}^2 - 2\,\mathbf{k}\,\mathbf{q}\right)^2} \tag{6.15}$$

is the dimensionless integral that in the nonrelativistic limit is equal to:

$$I\phi(q,\mathrm{v}<<c,\omega,\theta) \cong \frac{1+\cos^2\theta}{2} + \left(\frac{\omega}{q\,\mathrm{v}}\right)^2\,\frac{1-3\cos^2\theta}{2}, \tag{6.16}$$

θ is the angle between the IP velocity vector and the wave vector of a bremsstrahlung photon (the radiation angle).

In contrast to coherent radiation (Eq. 6.13), incoherent PBs (Eq. 6.14) is proportional to the concentration of medium atoms in the first degree and grows with the parameter u.

With the use of the formulas for the cross-section of atom-atom PBs given in [2, Chap. 7] it is possible to obtain the following equation for the number of photons of coherent PBs in a single crystal by the second channel (Fig. 6.1b):

$$\frac{dN_{proj}^{(coh)}}{dl\,d\omega\,d\Omega_{\mathbf{k}}} = \frac{n_t^2\,e^2Z_t^2}{\pi\,\hbar\,\mathrm{v}\,c^3}\left(1+\cos^2\theta_c\right)\sum_{\mathbf{g}}S^2(\mathbf{g})\;\delta(\omega+\mathbf{g}\mathbf{v}-\mathbf{k}\mathbf{v})\,\omega\,\omega_c^2$$
$$\times\left|\alpha_{proj}(\omega_c)\right|^2\,\exp\left(-u^2\,g^2\right)F_{proj}^2(\mathbf{g}_{1c})\left[1-\tilde{F}_t(g)\right]^2/g^2, \tag{6.17}$$

where Z_t is the charge number of nuclei of medium atoms. Appearing in the formula (6.17), in contrast to coherent PBs by the first channel, is the dynamic polarizability of the IP electron core $\alpha_{proj}(\omega_c)$ at the photon frequency in the reference system connected with an incident particle:

$$\omega_c = \gamma\,\omega\,(1 - (\mathrm{v}/c)\,\cos\theta), \tag{6.18}$$

where $\gamma = 1/\sqrt{1-(\mathrm{v}/c)^2}$. is the Lorentz factor. The expression (6.17) includes also the cosine of the angle of photon emission in the IP reference system:

$$\cos\theta_c = \frac{\cos\theta - \mathrm{v}/c}{1 - (\mathrm{v}/c)\,\cos\theta}. \tag{6.19}$$

The formula for incoherent PBs by the second channel looks like:

$$\frac{dN_{proj}^{(incoh)}}{dl\,d\omega\,d\Omega_{\mathbf{k}}} = Z_t^2 n_t\,\frac{e^2}{\hbar\,\omega}\,\frac{\left|\omega\,\omega_c\,\alpha_{proj}(\omega_c)\right|^2}{\pi\,\mathrm{v}^2\,c^3}\left(1+\cos^2\theta_c\right) \times \int\limits_{q_{\min}}^{q_{\max}} F_{proj}^2(q_{1c})\left[1-\tilde{F}_t(q)\right]^2\left(1-\exp\left(-u^2\,q^2\right)\right)\frac{dq}{q}. \tag{6.20}$$

It should be noted that the form factors of medium atoms and IP are included in the formulas (6.17), (6.20) for the second PBs channel differently than in the analogous expressions (6.13), (6.14) for the first channel, which reflects the distinction in the processes of radiation by these channels (see Fig. 6.1).

The appreciable difference between the coherent and incoherent PBs channels is that in the coherent case the radiation frequency is fixed for specified IP velocity, angle of photon emission, and reciprocal lattice vector. This fact manifests itself in the presence of a delta function in the formulas (6.13), (6.17), whence the equation for the coherent radiation frequency ("coherent" frequency) follows:

$$\omega_{\mathbf{g}}(\mathbf{N}) = \frac{-g_0\mathbf{N}\mathbf{v}}{1-(\mathrm{v}/\mathrm{c})\cos\theta}, \tag{6.21}$$

where the integer vector $\mathbf{N} = (N_1, N_2, N_3)$ is introduced that is related to the reciprocal lattice vector by the formula $\mathbf{g} = g_0\,(N_1, N_2, N_3)$, where $g_0 = 2\,\pi/d$ (d is the lattice constant).

Since in the experiment the recording of photons is carried out with the use of a photodetector with a finite frequency resolution, let us integrate the obtained

expressions for coherent PBs (6.13), (6.17) using the spectral function of the photodetector that we will choose in the form [8]:

$$f_{sp}(\omega) = \frac{1}{\sqrt{\pi}} \exp\left(-\frac{(\omega - \omega_r)^2}{\Delta\omega^2} \right), \tag{6.22}$$

where $\omega_r = r\,\varepsilon$ is the central frequency of the rth channel, $\Delta\omega$ is the spectral resolution of the photodetector ($\varepsilon < \Delta\omega$).

After the said frequency integration we obtain the following expression for coherent PBs by the first channel (see Fig. 6.1) recorded in the rth channel of the photodetector [12]:

$$\left(\frac{dN_t^{(coh)}}{dl\, d\Omega_{\mathbf{k}}} \right)_r \cong \frac{n_t^2\, e^2}{\pi\, \sqrt{\pi}\, \hbar\, \mathrm{v}\, c^3} \sum_{\mathbf{N}} S^2(\mathbf{N})\, \omega_{\mathbf{g}}^{\mathbf{3}}(\mathbf{N}) \left| \alpha_t\big(\omega_{\mathbf{g}}(\mathbf{N})\big) \right|^2 \exp\Big(-(u\, g_0)^2\, \mathbf{N}^2 \Big)$$
$$\times \exp\left(-\frac{\big(\omega_r - \omega_{\mathbf{g}}(\mathbf{N})\big)^2}{\Delta\omega^2} \right) \tilde{F}_t^2(g_0|\mathbf{N}|) \left[Z_{proj} - F_{proj}(g_0|\mathbf{N}|) \right]^2$$
$$G(\mathbf{s}, \mathbf{v}, \mathbf{N}, g_0)\, \Theta(-\mathbf{v}\mathbf{N}), \tag{6.23}$$

$$G(\mathbf{s}, \mathbf{v}, \mathbf{N}, g_0) = \frac{\left[\mathbf{s},\, \omega_{\mathbf{g}}(\mathbf{N})\, \mathbf{v}/c^2 - g_0\, \mathbf{N} \right]^2}{\left(g_0^2\, \mathbf{N}^2 - 2\, g_0\, \omega_{\mathbf{g}}(\mathbf{N})\, (\mathbf{s}\, \mathbf{N}) \right)^2}, \tag{6.24}$$

and $\Theta(-\mathbf{v}\mathbf{N})$ is the Heaviside step function providing the positiveness of frequency of an emitted photon.

The expression for coherent PBs by the second channel integrated with the use of the spectral function of the photodetector (Eq. 6.22) looks like:

$$\left(\frac{dN_{proj}^{(coh)}}{dl\, d\Omega_{\mathbf{k}}} \right)_r = \frac{Z_t^2\, n_t^2\, e^2}{\pi\sqrt{\pi}\, \hbar\, \mathrm{v}\, c^3} \frac{g_0\, \gamma^2}{1 - (\mathrm{v}/c)\cos\theta} \left(1 + \cos^2\theta_c \right)$$
$$\sum_{\mathbf{N}} S^2(\mathbf{N})\ \ \Theta(-\mathbf{v}\mathbf{N})\, (-\mathbf{v}\mathbf{N})^3 \times \left| \alpha_{proj}(-\gamma\, g_0\, \mathbf{v}\mathbf{N}) \right|^2$$
$$\exp\Big(-(u\, g_0)^2\, \mathbf{N}^2 \Big)\ \exp\left(-\frac{\big(\omega_r - \omega_{\mathbf{g}}(\mathbf{N})\big)^2}{\Delta\omega^2} \right)$$
$$\times F_{proj}^2(g_{1c}) \left[1 - \tilde{F}_t(g_0 N) \right]^2 / \mathbf{N}^2. \tag{6.25}$$

Here the photon frequency in the reference system connected with an IP in the argument of the dynamic polarizability of an IP is written out in the explicit form in view of the Eqs. 6.18 and 6.21. In the formulas (6.23), (6.25) summation over the

reciprocal lattice vectors are replaced by summation over the components of the integer vector $\mathbf{N} = (N_1, N_2, N_3)$.

For incoherent PBs by the second channel after frequency integration with the spectral function of the photodetector (6.22) the following approximate expression can be obtained:

$$\left(\frac{dN_{proj}^{(incoh)}}{dl\, d\Omega_{\mathbf{k}}}\right)_r \approx \frac{Z_t^2 n_t e^2}{2\sqrt{\pi}\hbar\, c}\left(\frac{c}{\mathrm{v}}\right)^2 \frac{(1+\cos^2\theta_c)\, r_e^2}{\gamma^2(1-(\mathrm{v}/c)\cos\theta)^2} \sum_n \frac{\omega_n}{\Delta\omega_n} f_n^2$$
$$\times \exp\left\{-\frac{\left[\omega_r - \omega_n^{(lab)}(\mathrm{v},\theta)\right]^2}{\Delta\omega^2}\right\} \int\limits_{\omega_n/\gamma\,\mathrm{v}}^{2\mu\mathrm{v}} \left(1-\exp\left(-q^2u^2\right)\right)$$
$$F_{proj}^2(q_{1c})\left[1-\tilde{F}_t(q)\right]^2 dq/q, \tag{6.26}$$

where $\omega_n^{(lab)}(\mathrm{v},\theta) = \frac{\omega_n}{\gamma(1-(\mathrm{v}/c)\cos\theta)}$ is the IP eigenfrequency in the laboratory reference system connected with a target, $r_e = e^2/mc^2$ is the electron classical radius. The derivation of the formula (6.26) was carried out under the assumption that $\Delta\omega_n << \Delta\omega$ ($\Delta\omega_n$ is the spectral width of the line of the bound-bound transition in the electron core of an IP). Besides, in Eq. 6.26 the cross terms appearing in squaring the magnitude of the IP polarizability are omitted. For the polarizability of a bound electron the following standard expression is used:

$$\alpha_{proj}(\omega_c) = \frac{e^2}{m}\sum_n \frac{f_n}{\omega_n^2 - \omega_c^2 - i\,\omega_c\,\Delta\omega_n}, \tag{6.27}$$

where f_n, ω_n are the oscillator strengths and the eigenfrequencies of transitions of a bound electron of an IP from the ground state to the exited states. We assume that the IP core during the process is invariably in the 1 s-state.

The spectral dependence of incoherent "target" PBs (the first channel) is rather weak, so integration of its spectrum with the tool function of the photodetector (Eq. 6.22) will result in multiplication of the primary expression (6.14) by the parameter $\Delta\omega$.

Let us use the obtained formulas for calculation of spectral, velocity (on the IP velocity), and angular dependences of four kinds of PBs arising in scattering of a hydrogen-like Ar^{17+} argon ion in a silicon single crystal. In this case for the geometrical structure factor of the crystal the equation is true [13]:

$$S(\mathbf{g}) = \frac{1}{4}\cos\left[\frac{\pi}{4}(N_1+N_2+N_3)\right]\{1+\cos(\pi N_1)+\cos(\pi N_2)+\cos(\pi N_3)\}, \tag{6.28}$$

where N_j are the integers that mark out nonzero terms in the sum over $\mathbf{N}$ in the expression for coherent PBs (6.23), (6.25).

For the parameters of the polarizability of a bound electron of an IP being in the ground 1s-state and of its form factor we use the known hydrogen-like formulas [14]:

$$\omega_n = Z_{proj}^2 \frac{n^2-1}{2\,n^2} \text{ a.u.}, \; f_n = n^5 \frac{2^8\,(n-1)^{2n-4}}{3\,(n+1)^{2n+4}}, \tag{6.29}$$

$$F_{proj}(q_1) = \frac{1}{\left(1+\left(a_{proj}\,q_1/2\right)^2\right)^2}, \; a_{proj} = \hbar^2/\left(Z_{proj}\,m\,e^2\right). \tag{6.30}$$

In the formulas (6.29) n is the principal quantum number of the electron core of an IP. Fine splitting of energy levels is neglected. To be specific, in calculations the natural broadening of transitions of an IP electron in the discrete spectrum is assumed, then

$$\Delta\omega_n = A_n = Z_{proj}^4 \frac{2^7\,n\,(n-1)^{2n-2}}{9\,c^3\,(n+1)^{2n+2}} \text{ a.u.}, \tag{6.31}$$

where A_n is the Einstein coefficient for a spontaneous transition.

It should be noted that using the formulas (6.29) that take into account only transitions in the discrete spectrum is justified by the fact that the contribution of the second PBs channel from bound-free transitions in the IP core is small.

The calculation of the dynamic polarizability and form factors of target atoms is described in detail in the work [5].

Presented in Fig. 6.7 are the dependences of four kinds of PBs at the central frequency of the photodetector ω_r calculated by the formulas of the previous section for a case of scattering of a hydrogen-like Ar^{17+} argon ion (the IP velocity v =4 6.65 a.u.) incoming along the crystallographic axis 2 (the input angle $\alpha = 0$, see Fig. 6.2) into a silicon single crystal. For short, we will call these dependences spectral. The radiation angle θ is supposed to be 120°, and the spectral resolution of the photodetector is taken equal to 3 a.u. ($\Delta\omega$=81.6 eV). From the figure it follows that the spectra of coherent PBs by the first and second channels are sets of maxima, the position of which, according to the formula (6.21), is defined by the reciprocal lattice vector transferred from an IP to the target during PBs, by the IP velocity and the radiation angle. The width of these spectral maxima is connected with the width of the spectral resolution of the photodetector $\Delta\omega$, and the value is defined by the magnitude of the polarizability of target atoms and an IP electron at the coherent frequency (6.21).

The spectrum of incoherent PBs by the second channel is defined by the spectral dependence of the IP polarizability having sharp peaks at frequencies that in the IP reference system are close to the eigenfrequencies of excitation of a bound electron

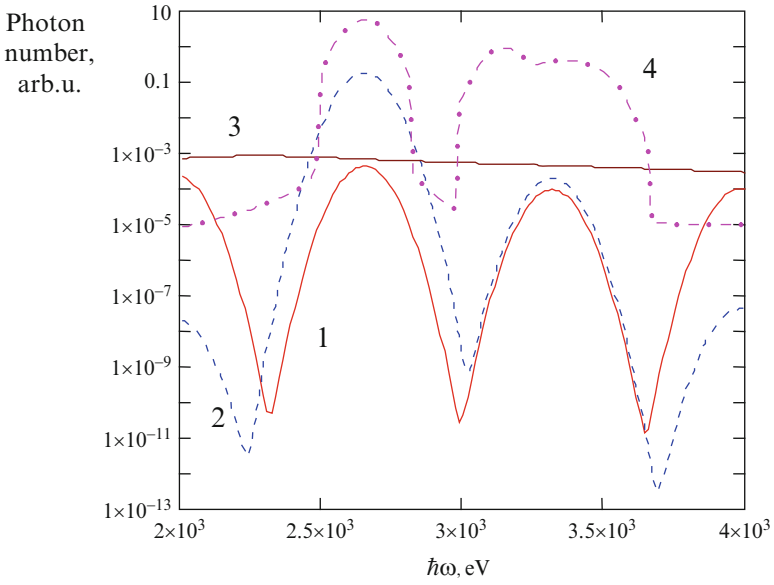

Fig. 6.7 The dependence of four kinds of PBs on photon energy at the central frequency of the photodetector in scattering of a hydrogen-like argon ion in a silicon single crystal (the ion velocity $v = 46.65$ a.u., the radiation angle $\theta = 120°$, the IP input angle $\alpha = 0$, the resolution of the photodetector $\Delta\omega$=81.6 eV): *1* – coherent PBs on a target, *2* – coherent PBs on an IP, *3* – incoherent PBs on a target, *4* – incoherent PBs on an IP

of a hydrogen-like ion. A corresponding condition for the frequency of a maximum in the spectrum of incoherent PBs by the second channel looks like:

$$\omega_{\max}(n, v, \theta) = \frac{\omega_n}{\gamma\,(1 - (v/c)\,\cos\theta)}. \tag{6.32}$$

The formula (6.32) is a condition of coincidence of the eigenfrequency of a bound electron of an IP in the laboratory reference system with the frequency of PBs recording. Owing to the Doppler effect, the eigenfrequency of the electron core of an IP in the laboratory system depends on the IP velocity and the radiation angle. The width of the discussed maxima, as in the coherent case, is defined by the value of the spectral resolution of the photodetector $\Delta\omega$.

It should be noted that in case of fast enough ions, following from the expression (6.32) is a possibility of radiation frequency tuning at the expense of change of the radiation angle, which may be found to be rather essential in practical applications of the phenomenon under consideration.

The spectrum of incoherent PBs by the first channel in the frequency range under consideration is described by a line weakly decreasing with growing frequency, close to the horizontal straight line. This is connected with the fact that the dynamic polarizability of target atoms defining this kind of PBs according to the formula

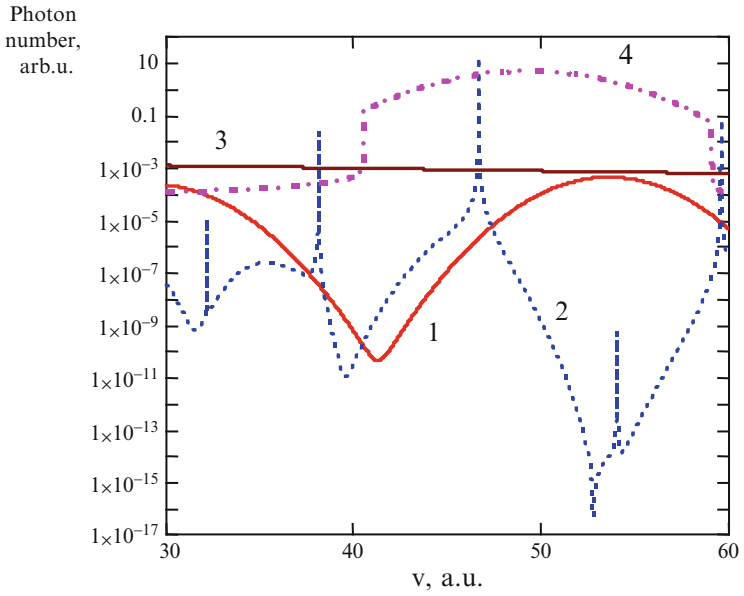

Fig. 6.8 The dependence on the velocity of an incident particle for four kinds of PBs in scattering of a hydrogen-like argon ion in a silicon single crystal (the photon energy at the central frequency of the photodetector $\hbar\omega_r = 2{,}448$ eV, the radiation angle $\theta = 135$, the IP input angle $\alpha = 0$, the resolution of the photodetector $\Delta\omega = 81.6$ eV): *1* – coherent PBs on a target, *2* – coherent PBs on an IP, *3* – incoherent PBs on a target, *4* – incoherent PBs on an IP

(6.14) depends rather weakly on the frequency in the spectral range presented in Fig. 6.7.

Figure 6.8 demonstrates the dependence of four kinds of PBs under consideration on the IP velocity for the bremsstrahlung photon energy at the central frequency of the photodetector $\hbar\omega_r = 2{,}445$ eV and a radiation angle of 135°. The input angle is supposed to be equal to zero, and the spectral width of the line of the photodetector resolution $\Delta\omega = 81.6$ eV.

From the figure it is seen that incoherent PBs by the first channel weakly depends on velocity. The velocity dependence of coherent PBs of the same channel is defined by the condition of equality of the frequency of recording the radiation and frequency of coherent radiation (Eq. 6.21). The maxima of the discussed dependence are connected with different reciprocal lattice vectors transferred from an IP to the target during coherent PBs. The width of these maxima is defined by the width of the spectral function of the photodetector (Eq. 6.22), and the value is defined by the dynamic polarizability of target atoms at the coherent frequency (6.21). It is seen that in the presented range incoherent PBs by the first channel everywhere prevails over coherent PBs.

The velocity dependence of incoherent PBs by the second channel has a wide maximum caused by the Doppler effect and the finite width of the spectral line of the photodetector. This maximum is connected with the fact that in view of fulfilment of

the condition $\Delta\omega_n << \Delta\omega$ the radiation frequency in the reference system connected with an IP is fixed and equal to one of the eigenfrequencies of a bound electron of an ion. When going to the laboratory reference system, the dependence of this resonance frequency on the IP velocity and the radiation angle appears, resulting in this maximum. The presented reasoning immediately follows from the expression (6.26).

A characteristic feature of Fig. 6.8 is the presence of sharp peaks in the velocity dependence of coherent PBs by the second channel. These peaks appear in case of equality of the coherent frequency (6.21) and one of the eigenfrequencies of a bound electron of an IP (the first equation in Eq. 6.29) converted to the laboratory reference system. This condition looks like:

$$\omega_{\max}(n, \mathrm{v}, \theta) \equiv \frac{\omega_n}{\gamma\,(1 - (\mathrm{v}/c)\,\cos\theta)} = \omega_{\mathbf{g}}(\mathbf{N}) \equiv \frac{-g_0 \mathbf{N}\mathbf{v}}{1 - (\mathrm{v}/\mathrm{c})\cos\theta}. \tag{6.33}$$

Hence the condition for the velocity value at the maximum of the velocity dependence follows:

$$\mathrm{v}_{\max}(n, \mathbf{N}, \alpha, \varphi) = \frac{c}{\sqrt{1 + \left(\frac{2\pi c}{\omega_n d}\right)^2 \left[N_1\,\sin\alpha\,\cos\varphi + N_2\,\sin\alpha\,\sin\varphi - N_3\,\cos\alpha\right]^2}}. \tag{6.34}$$

It should be noted that the velocity at the maximum does not depend on the angle of bremsstrahlung photon emission. In case of IP incoming along the crystallographic axis of the target ($\alpha = 0$) the expression (6.34) is simplified: the dependence only on the integer N_3 connected with the value of the transferred reciprocal lattice vector and on the eigenfrequency of an ion electron remains.

For maxima defined by the first eigenfrequency of an Ar^{17+} ion ($\omega_{n=2} = 3305$eV), from the Eq. 6.34 it is possible to obtain the table of values of IP velocity at the maxima of the velocity dependence of coherent PBs by the second channel (see Table 6.1).

Given in the second line of Table 6.1 are the values of coherent frequency (6.21) calculated for a radiation angle of 135°. The distinction of these values from the first eigenfrequency of an Ar^{17+} ion is connected with the Doppler effect.

In Fig. 6.8 four maxima corresponding to the values of IP velocity are well visible that are given in Table 6.1: 38.13, 46.656, and 59.579 a.u.. Also present in this figure are additional maxima of lesser values that are connected with equality of the coherent frequency (6.21) and other eigenfrequencies of the electron core of an IP (at $n>2$). The lesser value of these maxima is explained by the lesser value of oscillator strengths for virtual transitions to bound states of an IP electron with $n>2$.

The width of "velocity" maxima, as seen from Fig. 6.8, is rather small. It is defined by the value of spectral broadening of the line of the electron transition in the IP core that in the present calculation is supposed to be natural (see Eq. 6.31).

Table 6.1 Coherent frequency as a function of velocity in maximum for various N3 values

N_3	1	2	3	4	5
v_{max}, a.u.	112.751	80.372	59.579	46.656	38.13
$\hbar\omega_{\mathbf{g}}$, keV	1,187	1,892	2,276	2,505	2,652

Taking into account the additional mechanisms of broadening will result in broadening of corresponding velocity dependences.

From Fig. 6.8 it follows that for the parameters under consideration in the range of low velocities ($v < 42$ a.u.) incoherent Bs by the first channel prevails. For high IP velocities the main contribution to the process is made by incoherent PBs by the second channel, with the exception of rather narrow ranges near the values given in Table 6.1, where coherent PBs by the second channel prevails.

It should be noted that now rather high energy monochromaticity of an ion beam is achievable, at which the relative spread of IP velocity is fractions of a percent [1]. Therefore averaging over the spread of velocities in an ion beam should retain the main conclusions following from the given analysis of velocity dependences of different PBs kinds.

Presented in Fig. 6.9 are the angular dependences of considered kinds of PBs of an Ar^{17+} ion incoming into a silicon single crystal at a zero angle to the crystallographic axis for the IP velocity $v = 46.65$ a.u. and the bremsstrahlung photon energy $\hbar\omega_r = 2{,}448$ eV. The angular dependence of incoherent PBs by the first channel is manifested rather weakly.

The angular distributions of coherent PBs by both channels are similar: they have two maxima, and for wide angles maxima are more flat. The widths of these maxima are defined by the spectral resolution of the photodetector: they grow with $\Delta\omega$. Incoherent PBs by the second channel has a maximum in the region of wide radiation angles connected with fulfilment of the resonant condition in the polarizability of the electron core of an IP, when the conversion of the eigenfield of a target to a bremsstrahlung photon on a bound electron of an IP proceeds most effectively. On the whole, for specified values of IP velocity and bremsstrahlung photon energy incoherent PBs prevails in the angular dependence, and only in a rather narrow range of radiation angles near $\theta = 82^\circ$ prevailing is the contribution of coherent PBs by the first channel.

From the form of the angular dependences in Fig. 6.9 it follows that integration of the obtained expressions for PBs with the angular tool function of the photodetector may not change significantly the obtained result.

With increasing charge of the nucleus of a hydrogen-like ion the contribution of the second PBs channel to total radiation will decrease. This is connected, first, with growth of the IP eigenfield, which increases PBs by the first channel (see Eqs. 6.13, 6.14), and, second, with reduction of the polarizability of a bound electron of an IP. Really, in case of the natural broadening of the line (6.31) the sum over the principal quantum number in the formula (6.26) will contain the multiplier f_n/ω_n decreasing as Z_{proj}^{-2}. On the other hand, with growing Z_{proj} the spectral region of essentiality of PBs by the second channel will be shifted to the high-frequency region because of growing resonance frequencies of the polarizability of a hydrogen-like ion, whereas for low Z_{proj} this region

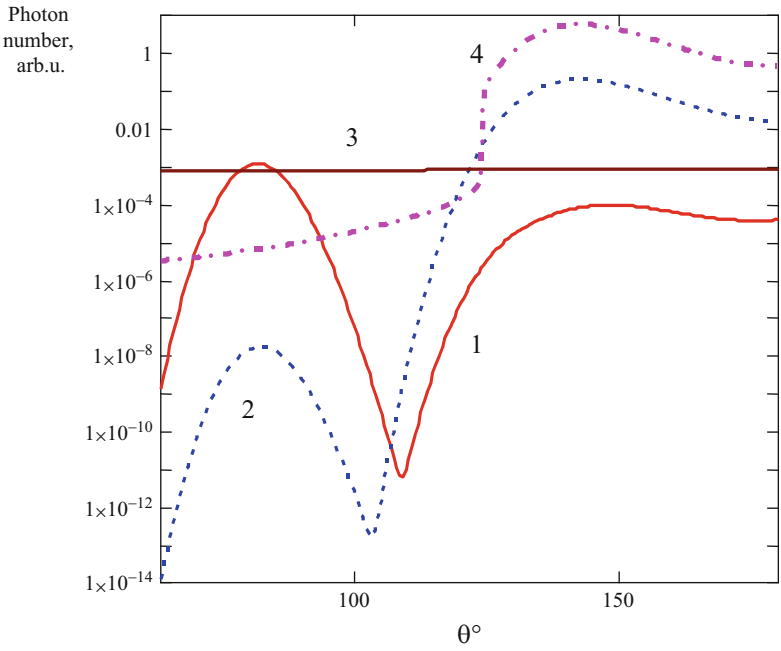

Fig. 6.9 The angular dependence of different kinds of PBs in scattering of a hydrogen-like argon ion in a silicon single crystal (the ion velocity v = 46.65 a.u., the photon energy $\hbar\omega_r$ = 2,448 eV, the input angle $\alpha = 0$, the resolution of the photodetector $\Delta\omega = 81.6$ eV): *1* – coherent PBs on a target, *2* – coherent PBs on an IP, *3* – incoherent PBs on a target, *4* – incoherent PBs on an IP

corresponds to vacuum ultraviolet radiation and soft X-rays. With growing charge of the nuclei of target atoms the relative contribution of the first and second PBs channels practically will not change, and radiation by each of the channels will increase proportionally.

6.2 Polarization Bremsstrahlung of a Fast Ion with an Electron Core in Plasma

In this paragraph within the framework of the first Born approximation polarization bremsstrahlung of a fast hydrogen-like ion in plasma is calculated and analyzed. The contribution of two channels to the process is taken into account: Eq. 6.35 of radiation due to conversion of the electromagnetic field of an ion to a real photon on plasma electrons and Eq. 6.36 of radiation as a result of virtual excitation of a bound electron of an ion (see Fig. 6.1a, b).

It is shown that the second channel of polarization bremsstrahlung has sharp peaks in the narrow spectral-angular range near the eigenfrequencies of the electron core of a fast ion, the spectral-angular dependence of radiation significantly depending on the velocity of an incident particle. The influence of plasma parameters on both polarization bremsstrahlung channels was investigated.

PBs of fast charged particles in plasma called transient Bs was for the first time investigated in the works of V.N. Tsytovich and A.V. Akopyan [15]. Further it was shown that this type of radiation is analogous to Bs in case of collision of charged particles with an atom that is caused by a variable dipole moment induced in the electron core of the atom by a scattered charged particle [2, Chap. 6]. PBs can arise also as a result of collision of neutral atoms or ions having an electron core. Then two channels of radiation are possible according to in which electron shell a radiating dipole moment is induced. Corresponding formulas for cross-sections in nonrelativistic and relativistic cases were obtained by M.Ya. Amus'ya with co-authors [2, Chap. 9].

Let us consider the process of emission of a transverse photon in scattering in plasma of an ion having a subsystem of bound electrons. By a transverse photon is meant the transverse mode of an electromagnetic field in plasma propagating also in vacuum in contrast to the longitudinal mode (plasmon). We assume that the ion velocity exceeds significantly the characteristic velocities of plasma particles and that the condition of the Born approximation for interaction of an IP with plasma particles is satisfied. Besides, we consider that the photon frequency $\omega > \gamma\,\omega_p$ (γ is the Lorentz factor of the IP, ω_p is the plasma frequency), then the influence of the density effect on Bs can be neglected.

As was already noted, the ordinary mechanism of Bs caused by acceleration of an IP in the target field is suppressed because of the high mass of an ion. As a result, the main radiative process is connected with the polarization mechanism of Bs. PBs in the case under consideration can proceed by two channels: (6.35) due to scattering of the IP eigenfield to a real photon on plasma electrons and Eq. 6.36 as a result of conversion of the eigenfield of plasma charges to a real photon on bound electrons of an IP. In both cases the energy of electromagnetic radiation is got from the kinetic energy of an IP, and the energy-momentum excess during the radiative process is absorbed by plasma ions. This interpretation assumes that the energy of plasma ions is insufficient to generate radiation of frequencies considered below.

6.2.1 *Polarization Bremsstrahlung Due to Virtual Excitation of Plasma Electrons (the First Channel)*

The expression for the differential cross-section of PBs in plasma by the first channel can be obtained within the framework of the approach described in [2, Chap. 6] that is based on the use of the formalism of the dynamic form factor of plasma components. The dimensionless PBs amplitude caused by the contribution of the jth plasma electron to the process under consideration is

$$T_{fi}^{PB} = 2\pi\, i\, \delta\left(\omega + \omega_{fi} + \mathbf{q}_1\mathbf{v}\right) \left(q_1^0\right)^2 \sqrt{\frac{2\,\pi}{\hbar\,\omega\,c^2\,V}}\, \frac{e^2}{m\,\omega^2} \left(\mathbf{e}_{\mathbf{k},\sigma}^{*},\, \mathbf{A}^{(pr)}(q_1)\right) \exp\left(i\,\mathbf{q}\,\mathbf{r}_j\right), \tag{6.35}$$

where V is the volume of quantization, $\mathbf{v}$ is the IP velocity and charge, $\hbar q = \hbar(q^0, \mathbf{q})$ is the four-dimensional energy-momentum vector transferred to plasma, $\hbar\omega_{fi}$ is the energy of excitation of a plasma electron during Bs, $q_1 = q - k = (1/\hbar)\left\{\varepsilon_f - \varepsilon_i,\ \mathbf{p}_f - \mathbf{p}_i\right\}$ is the four-dimensional wave vector proportional to the change of the IP energy-momentum, $k = (\omega/c,\ \mathbf{k})$ is the four-dimensional wave vector of a bremsstrahlung photon, $\mathbf{e}_{\mathbf{k},\sigma}$ is the unit vector of photon polarization,

$$\mathbf{A}^{(pr)}(q_1) = \frac{4\pi\, c e_{pr}}{q_1^0\, V}\, \frac{\mathbf{v}\, q_1^0/c^2 + \mathbf{q}_1}{\left(q_1^0/c\right)^2 - \mathbf{q}_1^2}, \qquad q_1^0 = \mathbf{q}_1\mathbf{v} \tag{6.36}$$

is the vector-potential of the IP field, $e_{pr} = Z_{pr}e$ is the IP charge. The axial gauge of the electromagnetic field is used, in which the scalar potential is equal to zero.

Summing the amplitude (Eq. 6.35) over all final states of a plasma electron $|f\rangle$, plasma electrons in the volume of quantization and polarizations of a bremsstrahlung photon σ, we find the following expression for the number of bremsstrahlung photons emitted by the first channel per unit IP trajectory length to the range of wave vectors $d\mathbf{k}$:

$$\frac{dN_{t\,\mathrm{arg}}}{dl\, d\omega\, d\Omega_{\mathbf{k}}} = \frac{1}{\pi^2}\, r_e^2\, \frac{c}{\mathrm{v}}\, \frac{e^2}{\hbar\,\omega} \int \left(Z_{pr} - F_{pr}(\mathbf{q})\right)^2 \frac{\left[\mathbf{s}, \omega\,\mathbf{v}/c^2 - \mathbf{q}\right]^2}{\left(\mathbf{q}^2 - 2\ \mathbf{k}\,\mathbf{q}\right)^2}\, S^{(ee)}\left(q^0, \mathbf{q}\right) d\mathbf{q}, \tag{6.37}$$

where Z_{pr}, $F_{pr}(\mathbf{q})$ are the charge number and the electron form factor of an IP, $r_e = e^2/mc^2$ is the electron classical radius, $\mathbf{s}$ is the unit vector in the direction of photon emission,

$$S^{(jl)}(q) = \frac{1}{2\,\pi} \int\limits_{-\infty}^{\infty} dt\, e^{i\,q^0\,t} \left\langle \hat{n}^{(j)}(\mathbf{q}, t)\, \hat{n}^{(l)}(-\mathbf{q}) \right\rangle \tag{6.38}$$

is the dynamic form factor corresponding to absorption of the four-momentum $\hbar q = \hbar(q^0, \mathbf{q})$ by plasma through interaction of the plasma components j and l. (For more details of the DFF of plasma components, see Appendix 3.)

PBs by the first channel is defined by the electron–electron DFF:

$$S^{(ee)}(q) = S_e^{(ee)}(q) + S_i^{(ee)}(q). \tag{6.39}$$

The first summand in the electron DFF (6.39) describes processes with transfer of the energy-momentum excess to the electron subsystem of plasma, the second summand does the same for the ionic subsystem. In the first case the conversion of the IP eigenfield occurs on individual plasma electrons (the incoherent process), and in the second case the conversion occurs on the Debye sphere screening a

plasma ion (the coherent process). Further we will be interested in coherent PBs. A corresponding component of the dynamic form factor of plasma $S_i^{(ee)}(q)$ in the limit $v>>v_{Ti}$ can be represented as:

$$S_i^{(ee)}(q) \cong n_i Z_i^2 \left| \frac{1-\varepsilon^{l(e)}(q)}{\varepsilon^l(q)} \right|^2 \delta(q^0), \tag{6.40}$$

where Z_i, n_i are the charge number and the concentration of plasma ions, $\varepsilon^{l(e)}(q)$, $\varepsilon^l(q)$ are the longitudinal dielectric permittivities of an electron plasma component and of plasma as a whole. The delta function in the Eq. 6.40 describes the energy conservation law with neglected recoil of a plasma ion. The coherent nature of the process is reflected in the quadratic dependence of $S_i^{(ee)}(q)$ on the number of electrons in the Debye sphere equal to Z_i. In the case under consideration for a fast IP ($v>>v_{Te}>>v_{Ti}$) we have

$$\varepsilon^{l(e)}(q) \cong \varepsilon^l(q=(0,\mathbf{q})) = 1 + \frac{1}{r_D^2\,\mathbf{q}^2}, \tag{6.41}$$

where r_D is the Debye radius. Then

$$S_i^{(ee)}(q) \cong n_i \left| \frac{Z_i}{1+r_D^2\,\mathbf{q}^2} \right|^2 \delta(q^0) = n_i\, |F_i(\mathbf{q})|^2\, \delta(q^0). \tag{6.42}$$

Here the form factor of the Debye sphere screening an ion in plasma is introduced by analogy with the atomic case that is by definition equal to:

$$F_i(\mathbf{q}) = \frac{Z_i}{1+r_D^2\,\mathbf{q}^2}, \tag{6.43}$$

so the spatial Fourier transform of the charge of a plasma ion on the wave vector $\mathbf{q}$ in the units of elementary charge is $Z_i - F_i(\mathbf{q})$. Substituting the expressions (6.42), (6.43) in the formula (6.37) and dividing by the concentration of ions, we obtain the expression for the differential cross-section of PBs on the Debye sphere ("target" PBs) with transfer of the energy-momentum excess to a plasma ion:

$$\frac{d\sigma_{t\,\mathrm{arg}}^{PB}}{d\omega\, d\Omega_{\mathbf{k}}} = \frac{2Z_i^2}{\pi\,\omega}\,\frac{v_a\, c}{v^2}\, r_e^2 \int\limits_{q_{\min}}^{q_{\max}} \frac{\left(Z_{pr} - F_{pr}(\mathbf{q})\right)^2 I_\phi(q,v,\omega,\theta)\, dq}{\left(1+r_D^2\,q^2\right)^2 q}, \tag{6.44}$$

where $v_a = e^2/\hbar$, $q = |\mathbf{q}|$, $\theta = \mathbf{k}^\wedge\mathbf{v}$ is the radiation angle, and

$$I_\phi(q,v,\omega,\theta) = \frac{q^3\, v}{2\,\pi} \int d\Omega_{\mathbf{q}}\, \delta(\omega - \mathbf{k}\mathbf{v} + \mathbf{q}\mathbf{v})\, \frac{\left[\mathbf{s}, \omega\,\mathbf{v}/c^2 - \mathbf{q}\right]^2}{\left(\mathbf{q}^2 - 2\,\mathbf{k}\,\mathbf{q}\right)^2} \tag{6.45}$$

is the kinematic integral that in the nonrelativistic limit is

$$I_\phi(q, \mathrm{v}<<c, \omega, \theta) \cong \frac{1+\cos^2\theta}{2} + \left(\frac{\omega}{q\,\mathrm{v}}\right)^2 \frac{1-3\cos^2\theta}{2}. \tag{6.46}$$

6.2.2 *Polarization Bremsstrahlung as a Result of Virtual Excitation of the Electron Core of an IP (the Second Channel)*

For the differential cross-section of the second PBs channel with generalization of the formulas obtained by M.Ya. Amus'ya with co-authors [2, Chap. 9], in case of atom-atom and ion-ion collisions the following expression can be obtained:

$$\frac{d\sigma^{PB}_{proj}}{d\omega\, d\Omega_{\mathbf{k}}} = \frac{Z_i^2}{\pi} \frac{\mathrm{v}_a\, \omega\, \omega_c^2}{\mathrm{v}^2\, c^3} \left|\alpha_{proj}(\omega_c)\right|^2 \left(1+\cos^2\theta_c\right) I_{pl}(r_D), \tag{6.47}$$

where $\alpha_{proj}(\omega_c)$ is the dynamic polarizability of an incident particle,

$$\omega_c = \gamma\,\omega\,(1-(\mathrm{v}/c)\,\cos\theta),\ \cos\theta_c = \frac{\cos\theta - \mathrm{v}/c}{1-(\mathrm{v}/c)\,\cos\theta} \tag{6.48}$$

are the frequency and the cosine of the radiation angle in the reference system connected with an incident particle,

$$I_{pl}(r_D) = \int\limits_{r_D\, q_{\min}}^{r_D\, q_{\max}} \frac{x^3\, F_{pr}(x/r_D)\, dx}{\left(1+x^2\right)^2}, \tag{6.49}$$

$$q_{\min} = \frac{\omega}{\mathrm{v}}(1-(\mathrm{v}/\mathrm{c})\,\cos\theta),\ q_{\max} = \frac{2\,\mu\,\mathrm{v}}{\hbar}, \tag{6.50}$$

where μ is the reduced mass of an IP and a plasma ion. In derivation of the formula (6.47) the expression for the form factor of the Debye sphere (Eq. 6.43) was used, by which the above generalization of the formulas of the work [2, Chap. 9] to the plasma case is achieved.

Further we will consider a case of a *hydrogen-like* incident ion. Then for the dynamic polarizability of an IP we have:

$$\alpha_{proj}(\omega) = \frac{e^2}{m} \sum_n \frac{f_n}{\omega_n^2 - \omega^2 - i\omega\delta_n}, \tag{6.51}$$

where

$$\omega_n = Z_{pr}^2 \frac{Ry}{\hbar}\left(1 - \frac{1}{n^2}\right) \tag{6.52}$$

are the eigenfrequencies of a bound electron of an IP, f_n are the oscillator strengths, δ_n are the damping constants. A characteristic feature of the dynamic polarizability of a hydrogen-like ion is the presence of sharp resonances at $\omega \approx \omega_n$ since $\omega_n >> \delta_n$. The electron form factor for the ground state of a hydrogen-like IP is

$$F_{pr}(q) = \frac{1}{\left(1 + (a\,q/2)^2\right)^2}, \tag{6.53}$$

where $a = \hbar^2/\left(Z_{pr}\, me^2\right)$. Substituting Eq. 6.53 in the formula (6.49), we find

$$I_{pl}(r_D, a) = \int\limits_{r_D\, q_{\min}}^{r_D\, q_{\max}} \frac{x^3\, dx}{\left(1 + x^2\right)^2 \left(1 + (a/2\, r_D)^2\, x^2\right)^4}. \tag{6.54}$$

It should be noted that in the limit $r_D >> a$ characteristic for nondegenerate plasma the approximate equation is true:

$$I_{pl}(r_D >> a) \approx \ln\left(\frac{2\, r_D}{a\,\sqrt{1 + r_D^2\, q_{\min}^2}}\right) - \frac{17 + 11\, r_D^2\, q_{\min}^2}{12 + 12 r_D^2\, q_{\min}^2}. \tag{6.55}$$

The cross-section of ordinary Bs of an electron in plasma in the frequency range under consideration $m\,\mathrm{v}^2/2\,\hbar >> \omega > \gamma\,\omega_p$ can be obtained if in the formula (6.47) the function $\alpha_{proj}(\omega_c)$ is replaced by the dynamic polarizability of a free electron, and instead of the integral $I_{pl}(r_D)$, $\ln(m\,\mathrm{v}\, r_D/\hbar)$ is substituted. As a result, we find

$$\frac{d\sigma_e^{OB}}{d\omega\, d\Omega_{\mathbf{k}}} = \frac{Z_i^2}{\pi}\, r_e^2\, \frac{\mathrm{v}_a\, c}{\mathrm{v}^2}\, \frac{1 + \cos^2\theta_c}{\gamma^2\,(1 - (\mathrm{v}/c)\,\cos\theta)^2}\, \ln\left(\frac{m\,\mathrm{v}\, r_D}{\hbar}\right). \tag{6.56}$$

Now let us consider some limiting cases of the above expressions for the cross-sections of PBs by the first and second channels. In the nonrelativistic case (v) in the frequency range $\omega < \mathrm{v}/r_D$ the formulas (6.44), (6.46) give

$$\frac{d\sigma_{t\,\mathrm{arg}}^{PB}(\omega < \mathrm{v}/r_D)}{d\omega\, d\Omega_{\mathbf{k}}} = \frac{2Z_i^2}{\pi}\, \frac{\left(Z_{pr} - 1\right)^2}{\mathrm{v}^2\, c^3\, \omega}\, \left(1 + \cos^2\theta\right) \ln\left(\frac{\mathrm{v}}{\omega\, r_D}\right). \tag{6.57}$$

In the opposite case of high enough frequencies $\omega > \mathrm{v}/r_D$, for the differential cross-section by the first channel we have

$$\frac{d\sigma^{PB}_{t\,\mathrm{arg}}(\omega > \mathrm{v}/r_D)}{d\omega\, d\Omega_{\mathbf{k}}} = \frac{Z_i^2}{2\pi}\left(Z_{pr}-1\right)^2\left(1+\cos^2\theta\right)\frac{\mathrm{v}^2}{c^3\,\omega^5\,r_D^4}\,. \tag{6.58}$$

The obtained expression contains the small multiplier $(\mathrm{v}/\omega\, r_D)^4$ that describes the suppression of PBs on the Debye cloud in the frequency range under consideration. This suppression is connected with the loss of coherence of conversion of a virtual photon to a real photon on the electron charge of the Debye sphere if $\lambda < r_D$ (λ is the wavelength of a bremsstrahlung photon).

In the low-frequency limit $\omega < \mathrm{v}/r_D$ in case of nondegenerate plasma the inequation $\omega < Z_{pr}^2 Ry$ is satisfied. Then for the IP polarizability it is possible to use the static approximation that for a hydrogen-like ion gives $\alpha_{proj}(0) = a_B^3 \Big/ Z_{pr}^4$, where a_B is the Bohr radius. Substituting this expression in the formula for the cross-section of PBs by the second channel (Eq. 6.47), we obtain:

$$\frac{d\sigma^{PB}_{proj}\left(\omega < Z_{pr}^2 Ry\right)}{d\omega\, d\Omega_{\mathbf{k}}} = \frac{81}{4\pi}\frac{Z_i^2}{Z_{pr}^4}a_B^6\frac{\omega^3\,\mathrm{v}_a}{\mathrm{v}^2\,c^3}\frac{\left(1-(\mathrm{v}/c)\,\cos\theta\right)^2}{1-(\mathrm{v}/c)^2}\left(1+\cos^2\theta_c\right)\,\ln\!\left(\frac{r_D}{a}\right). \tag{6.59}$$

In case of fulfilment of the inequation $\delta_n << |\omega_c - \omega_n| << \omega_n$ for the dynamic polarizability of an IP the resonant approximation "works". Then for the differential cross-section of PBs by the second channel the formula is true:

$$\frac{d\sigma^{PB}_{proj}(\omega_c \approx \omega_n)}{d\omega\, d\Omega_{\mathbf{k}}} \cong \frac{Z_i^2}{2\pi}\frac{r_e^2}{\omega}\frac{\mathrm{v}_a\, c}{\mathrm{v}^2}\frac{f_n^2}{\left[\frac{\omega_n}{\omega}-\gamma\left(1-\frac{\mathrm{v}}{c}\cos\theta\right)\right]^2}\left(1+\cos^2\theta_c\right)I_{pl}(r_D), \tag{6.60}$$

following from which is the presence of sharp peaks in the frequency-angular PBs distribution caused by conversion of fluctuations of the electric field of plasma to a real photon on a bound electron of a hydrogen-like IP. The frequency of a peak depends on the angle of photon emission the and IP energy according to the equation:

$$\omega_{\max}(n,\mathrm{v},\theta) = \frac{\omega_n}{\gamma\left(1-(\mathrm{v}/c)\cos\theta\right)}. \tag{6.61}$$

At a fixed PBs frequency the maximum in the angular distribution of the process is defined by the angle

$$\theta_{\max}(n,\omega,\mathrm{v}) = \arccos\left\{\frac{c}{\mathrm{v}}\left(1-\frac{\omega}{\gamma\,\omega_n}\right)\right\}. \tag{6.62}$$

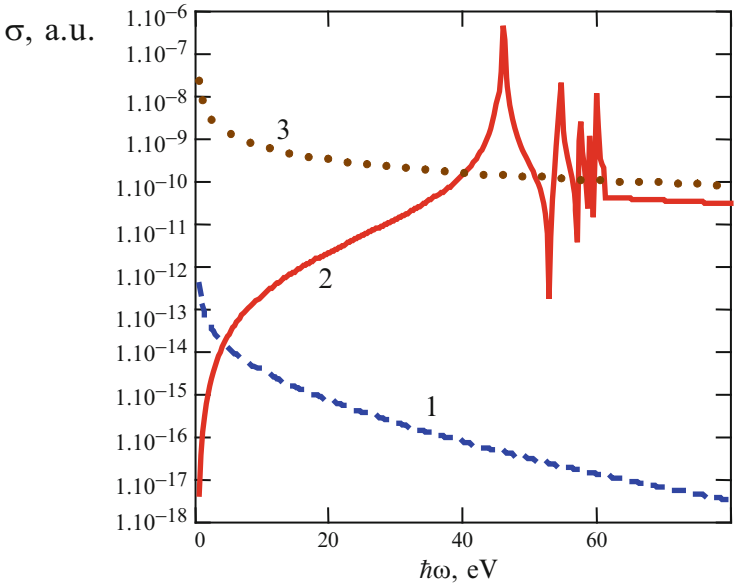

Fig. 6.10 The spectrum of PBs by the first channel (*curve 1*), by the second channel (*curve 2*) of a He^+ ion and the spectrum of ordinary Bs of an electron (*curve 3*) in nondegenerate plasma ($r_D = 5{\cdot}10^{-6}$ cm): v = $1.98{\cdot}10^{10}$ cm/s, $\theta = \pi/3$

From the Eq. 6.62 it follows in particular that the angular maximum occurs in fulfilment of the inequations

$$\gamma\left(1-\frac{\mathrm{v}}{c}\right)\omega_n \le \omega \le \gamma\left(1+\frac{\mathrm{v}}{c}\right)\omega_n. \tag{6.63}$$

Beyond the said spectral range the angular dependence of the cross-section of resonant PBs by the second channel has a monotonic behavior.

Calculated by the formulas (6.44), (6.47) the spectra of two PBs channels in scattering of a hydrogen-like helium ion (v = 90a.u.) in nondegenerate plasma ($r_D = 10^3$ a.u.) (curves 1, 2) are presented in Fig. 6.10 together with the spectrum of ordinary Bs of an electron (curve 3) for the radiation angle $\theta = \pi/3$.

It is seen that PBs caused by conversion of the electric field of a plasma ion on a bound electron of an IP to a bremsstrahlung photon (the second channel) has sharp maxima at frequencies described by the formula (6.61), corresponding to resonances of the dynamic polarizability of an IP. PBs by the second channel prevails everywhere, with the exception of the narrow region of low frequencies. At $\omega \to 0$ the spectral cross-section of the second channel decreases according to the formula (6.59) as the third power of frequency. At the same time the cross-section of the first PBs channel rapidly decreases with growing frequency because of the loss of coherence in reradiation of the IP eigenfield by electrons of the Debye sphere to a bremsstrahlung photon. This circumstance is connected with the high value of the

Debye radius in nondegenerate plasma $r_D >> a_B$, so the inequation $\omega > \mathrm{v}/r_D$ is satisfied in the overwhelming part of the spectral range, and the low value of the process cross-section in this case is predicted by the formula (6.58). Thus the spectral regions of essentiality of two PBs channels in nondegenerate plasma are much spaced due to the high value of the Debye radius. It should be noted that in the region of high frequencies, when the inequation $\omega_c > Z_{pr}^2 Ry$ is satisfied, the cross-sections of PBs of a hydrogen-like ion by the second channel and of ordinary Bs of an electron are close in value. This is connected with the fact that in the region of high frequencies the dynamic polarizability of an IP is close to that for a free electron.

With growing IP velocity the spectral maxima of PBs by the second channel are shifted to the region of lower frequencies, and the cross-section of the second channel decreases not so rapidly. Similar changes of the spectra occur with reduction of the radiation angle.

The spectral Bs cross-sections in scattering of a hydrogen-like carbon ion in degenerate plasma are presented in Fig. 6.11. Since in this case the Thomas-Fermi radius is much less than the Debye radius of nondegenerate plasma, the spectral ranges of essentiality of both PBs channels intersect. The second PBs channel, as before, prevails near the resonances of the dynamic polarizability of an IP.

The angular dependence of total PBs (the sum of both channels) in scattering of a hydrogen-like helium ion ($\mathrm{v} = 90$ a.u.) in nondegenerate plasma is presented in Fig. 6.12 for the frequency $\omega = 1.7$ a.u. (46.24 eV). From Fig. 6.12 it follows that the angular dependence of PBs of a hydrogen-like ion in plasma has sharp maxima corresponding, according to the formula (6.62), to the resonant condition $\omega_c(\mathrm{v},\theta) \approx \omega_n$ if only the frequency of a bremsstrahlung photon in the laboratory reference system satisfies the inequations (6.63). These maxima are shifted to the region of small angles with growing IP velocity.

The dependence of PBs of a hydrogen-like carbon ion scattered in nondegenerate plasma on the IP velocity is presented in Fig. 6.13 for two radiation angles: $\theta = \pi/10$ and $\theta = \pi/6$. The bremsstrahlung photon energy is $\hbar\omega = 544$ eV.

Two sharp peaks on these curves correspond to the resonance of the dynamic polarizability of a carbon ion in excitation of its bound electron from the ground state to the first exited condition. It is seen that with growing radiation angle the position of the maximum is shifted to the region of higher velocities.

This circumstance is a corollary of the formulas (6.52), (6.61) determining the photon energy at the maximum of the spectral dependence of the PBs cross-section as a function of the radiation angle and the IP velocity. Following from them is the expression for the IP velocity at the maximum:

$$\mathrm{v}_{\max}^{(\pm)} = c\,\frac{\cos\theta \pm \sqrt{\cos^2\theta + \left[(\omega_n/\omega)^2 - 1\right]\left[(\omega_n/\omega)^2 + \cos^2\theta\right]}}{(\omega_n/\omega)^2 + \cos^2\theta}, \qquad (6.64)$$

where ω_n is the eigenfrequency of a bound electron of an IP that is given by the formula (6.52). The expression (6.64), naturally, is true for $\mathrm{v}_{\max}$. Depending on the

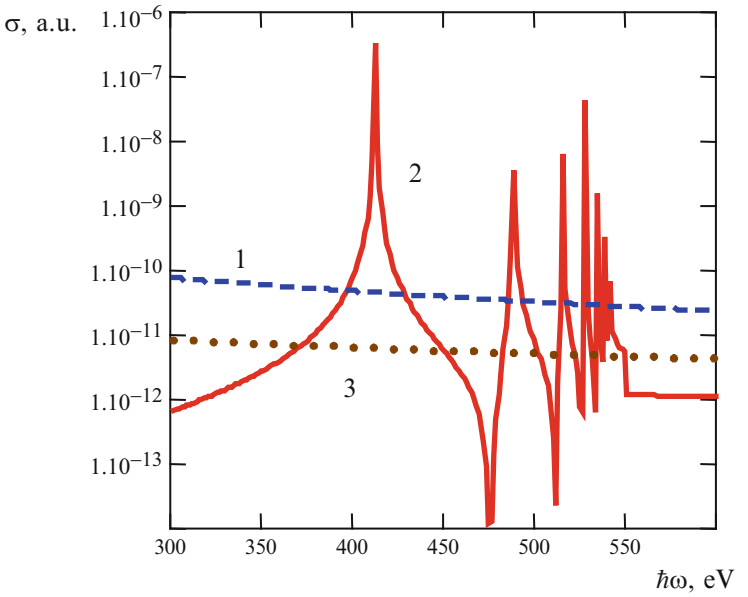

Fig. 6.11 The spectrum of PBs by the first channel (*curve 1*), by the second channel (*curve 2*) of a C^{+5} ion and the spectrum of ordinary Bs of an electron (*curve 3*) in degenerate plasma ($r_{TF} = 5{\cdot}10^{-9}$ cm): $v = 1.98{\cdot}10^{10}$ cm/s, $\theta = \pi/3$

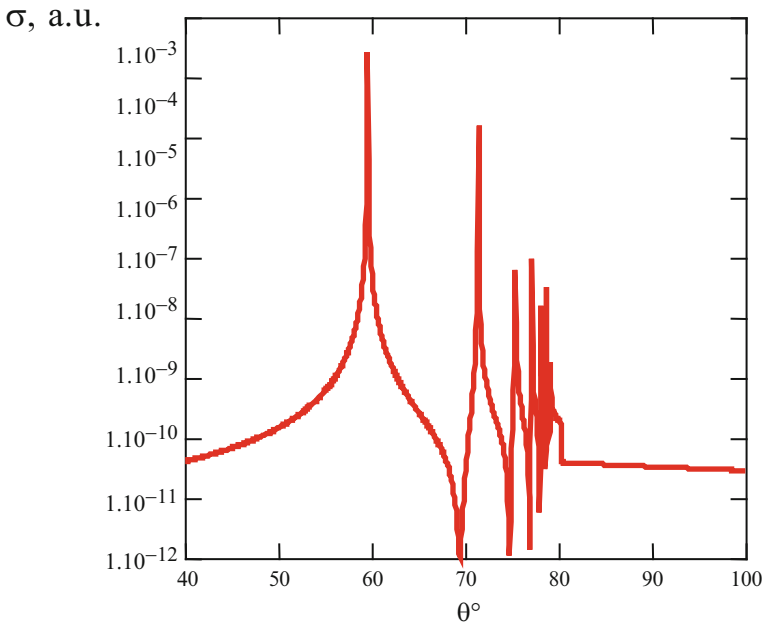

Fig. 6.12 The angular dependence of total PBs of a He^{+} ion ($v = 90$ a.u.) in nondegenerate plasma ($r_D = 5{\cdot}10^{-6}$ cm) for the bremsstrahlung photon energy $\hbar\omega = 46.24$ eV

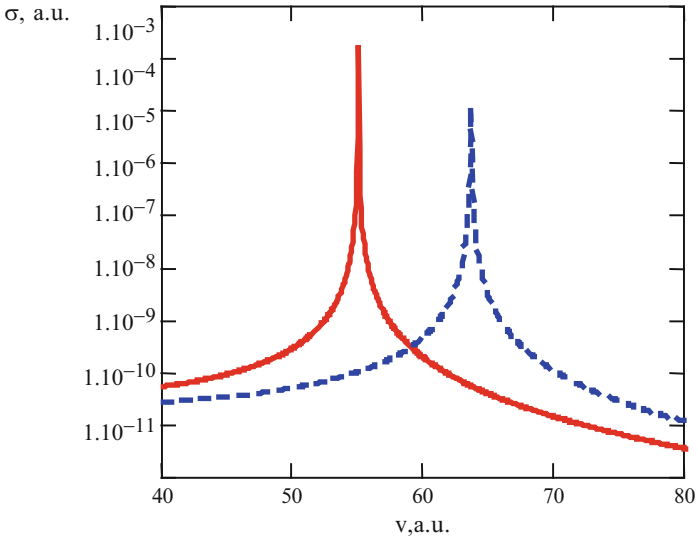

Fig. 6.13 The dependence of total PBs on the velocity of a C^{+5} ion ($\hbar\omega = 544$ eV) in nondegenerate plasma ($r_D = 5{\cdot}10^{-6}$ cm) for two radiation angles: *solid curve* – $\theta = \pi/10$, *dashed curve* – $\theta = \pi/6$

value of the ratio (ω_n/ω) and the radiation angle θ, the function $\sigma(v)$ can have two, one, or no maxima. For example, if the radicand on the right side of the Eq. 6.64 is equal to zero, it is obvious that $v_{max}^{(-)} = v_{max}^{(+)}$ – there is one maximum. Satisfying this condition is the relationship between the frequency and the radiation angle:

$$\omega = \frac{\omega_n}{\sin\theta} \equiv \omega^*. \tag{6.65}$$

In fulfilment of Eq. 6.65, following from Eq. 6.64 is a simple relation between the velocity at the maximum of the cross-section of PBs by the second channel and the radiation angle: $v_{max} = c\cos\theta$. At frequencies $\omega > \omega^*$ the PBs cross-section sharply decreases since the approximate equation $\omega_c \approx \omega_n$ resulting in a resonance in the dynamic polarizability of an IP ceases to be satisfied. With decreasing radiation frequency, when $\omega << \omega^*$, from the expression (6.64) the limiting dependences follow: $v_{max}^{(-)} \to 0$ and $v_{max}^{(+)} \to c$. Then the cross-section of PBs by the second channel is low in a wide range of IP velocities.

References

1. Eichler, J., Stöhlker, T.: Radiative electron capture in relativistic ion–atom collisions and the photoelectric effect in hydrogen-like high-Z systems. Phys. Rep. **439**, 499 (2007)
2. Tsytovich, V.N., Oiringel, I.M. (eds.): Polarization Bremsstrahlung. Plenum, New York (1991)

3. Nasonov, N.N.: Collective effects in the polarization bremsstrahlung of relativistic electrons in condensed media. NIM B **145**, 19 (1998)
4. Feranchuk, I.D., Ulyanenkov, A., Harada, J., Spencer, J.C.H.: Parametric x-ray radiation and coherent bremsstrahlung from nonrelativistic electrons in crystals. Phys. Rev. E **62**(4225) (2000)
5. Astapenko, V.A.: Polarization bremsstrahlung of heavy charged particles in polycrystal. JETP **99**, 958 (2004)
6. Astapenko, V.A., Buimistrov, V.M., Krotov, Y.A., Nasonov, N.N.: Polarization bremsstrahlung from non-relativistic electrons penetrating a polycrystalline target. Phys. Lett. A **332**, 298 (2004)
7. Astapenko, V.A., Nasonov, N.N.: Suppression of the polarization bremsstrahlung from a fast charged particle in an amorphous medium. JETP **103**, 553 (2006)
8. Baryshevsky, V.G., Batrakov, K.G., Feranchuk, I.D., et al.: Experimental observation of frequency tuning of x-ray radiation from nonrelativistic electrons in crystals. Phys. Lett. A **363**, 448 (2007)
9. Rzadkiewicz, J., Rosmej, O., Blazevic, A., et al.: Studies of the Kα X-ray spectra of low-density SiO_2 aerogel induced by Ca projectiles for different penetration depths. High Energy Density Phys. **3**, 233 (2007)
10. Hoffmann, D.H., Blazevic, A., Ni, P., et al.: Present and future perspectives for high energy density physics with intense heavy ion and laser beams. Laser Part. Beam. **23**, 47 (2005)
11. Azuma, T., Ito, T., Takabaysahi, Y., et al.: Resonant coherent excitation of hydrogen-like Ar ions to the n = 3 states. Physica Scripta **T92**, 61 (2001)
12. Astapenko, V.: Polarization bremsstrahlung from fast ions with the core in polycrystal. NIM B **266**, 3744 (2008)
13. Animalu, A.O.E.: Intermediate Quantum Theory of Crystalline Solids. Prentice-Hall, New Jersey (1978)
14. Bethe, H.A., Salpeter, E.E.: Quantum Mechanics of One and Two Electrons Atoms. Springer, Berlin (1957)
15. Tsytovich, V.N., Akopyan, A.V.: Bremsstrahlung in a nonequilibrium plasma. Sov. J. Plasma. Phys. **1**, 371 (1975)